Tropical Journal of Pharmaceutical Research July 2022; 21 (7): 1365-1375
ISSN: 1596-5996 (print); 1596-9827 (electronic)

Available online at http://www.tjpr.org
http://dx.doi.org/10.4314/tjpr.v21i7.2

Original Research Article

Optimization of process parameters by response surface methodology to develop a more bioefficacious nanosuspension of Silybum marianum seed extract

Fareeha Kousar[1]*, Nazish Jahan[1], Bushra Sultana[1], Khalil-Ur-Rahman[2]
[1]Department of Chemistry, [2]Department of Biochemistry, University of Agriculture, Faisalabad, Pakistan

For correspondence: **Email: fareehakousar87@gmail.com; **Tel:** +92-419200161*

Sent for review: 6 February 2020 *Revised accepted: 24 June 2022*

Abstract

Purpose: *To develop a nanosuspension drug delivery system to enhance the dissolution rate of Silybum marianum seeds extract.*
Methods: *Central composite design was used to study the effect of the input variables (stabilizer to plant extract ratio, antisolvent to solvent ratio, stirring time) on the dependent variables (mean particle size, polydispersity index (PDI) and zeta potential). The optimized formulation was characterized by Scanning Electron Microscopy (SEM), Atomic Force Microscopy (AFM), Fourier Transformed Infrared Microscopy (FT-IR) and in vitro dissolution testing.*
Results: *The optimized nanosuspension with mean particle size of 137 nm, PDI of 0.327 and zeta potential of -37 mV was obtained. SEM studies revealed irregular shaped particles. AFM studies showed nanosized particles with good surface characteristics. The optimized formulation showed faster dissolution rate than coarse suspension.*
Conclusion: *Results suggested that nanosuspension has remarkable potential for enhancement of the dissolution properties of poorly soluble S. marianum seed extract.*

Keywords: *Silybum marianum, Nanosuspension, Optimization, Dissolution rate*

Tropical Journal of Pharmaceutical Research is indexed by Science Citation Index (SciSearch), Scopus, Web of Science, Chemical Abstracts, Embase, Index Copernicus, EBSCO, African Index Medicus, JournalSeek, Journal Citation Reports/Science Edition, Directory of Open Access Journals (DOAJ), African Journal Online, Bioline International, Open-J-Gate and Pharmacy Abstracts

INTRODUCTION

Silybum marianum, commonly called milk thistle, is a plant of the Asteraceae family widely used as a therapeutic agent for a variety of diseases including liver diseases, colon and prostate cancer [1]. The purified mixture of flavonoids extracted from the seeds and flowers of *Silybum marianum* called silymarin. Silybin is the most active component of this mixture (comprised 60 – 70 % of the total content of silymarin) is responsible for most of its pharmacological activities [2].

Silybin is an important hepatoprotective flavonoid frequently used for the treatment of various hepatic disorders [3]. However, the clinical applications of silymarin are hindered due to its poor water solubility and low bioavailability [4]. The slightly soluble drugs presented limited dissolution rate in gastrointestinal fluid. Therefore, only a small concentration of the drug

becomes available at the target site and in situations where *in vivo* treatment fails. Thus, *in vitro* dissolution becomes an important factor in the development of new drugs and the enhancement of the dissolution velocity of poorly water-soluble drugs, to increase their bioavailability which is a challenging task for pharmaceutical preparation workers [5].

Nanosuspension is a carrier free drug delivery system, consisting of nanosized drug particles stabilized by polymers or surfactants [6]. nanosuspension is an ideal pharmaceutical formulation for increasing the solubility and dissolution of poorly water-soluble drugs and phytoconstituents [7]. The reduced particle size offers high surface area which dramatically increased the saturation solubility, dissolution velocity and ultimately translates into improved bioavailability of drug candidates [8]. Other potential advantages of nanosuspensions are high drug loading [9], rapid onset of action, dose reduction, reduced side effects, decreased fasted variability, better stability [10] and enhanced absorption [11]. Due to these unique advantages, nanosuspensions have become a choice of drug delivery system for the pharmaceutical industries and many nanosuspension formulations are now marketed [12]. In addition, various administration routes such as oral, parenteral, nasal, intravenous and pulmonary have been reported for nanosuspensions [13].

EXPERIMENTAL

Preparation of plant extract

Seeds of *S. marianum* were collected from the Natural Product Lab, Department of Chemistry, University of Agriculture, Faisalabad and identified by a plant taxonomist from the Department of Botany, University of Agriculture, Faisalabad. Seeds of *S. marianum* were first defatted with n-hexane to remove fatty substances, and the defatted plant material was extracted with ethanol. The ethanolic extract was concentrated using rotary evaporator.

Formulation of nanosuspension

Nanosuspension of *S. marianum* extract was prepared by antisolvent precipitation method. First, plant extract (200mg) was completely dissolved in ethanol which was termed as organic phase. This organic solution was slowly injected into aqueous phase containing sodium lauryl sulphate (SLS) as stabilizer with continuous stirring at mechanical stirrer. The mixture was continuously stirred for six hours at room temperature. The nanosuspension was filtered and stored in transparent plastic bottles [14].

Optimization of process parameters by response surface methodology

For optimization of the parameters of nanosuspensions, Central Composite Design (CCD) was used. Stabilizer to plant extract ratio (S/PE ration, A), antisolvent to solvent ratio (AS/S ration, B) and stirring time (C) were the independent variables, and mean particle size (Y_1), PDI (Y_2) and zeta potential (Y_3) were selected as response variables in this study.

Evaluation of nanosuspension stability

The physical stability of optimized nano-suspension was evaluated at two different temperatures. For this purpose, optimized nanosuspension was stored at 25 ºC (at room temperature) and 4 ºC (in refrigerator) for the period of three months. After three months aliquots of samples were drawn and analyzed for particle size, PDI and zeta potential.

Lyophilization of nanosuspension

Optimized nanosuspension were lyophilized to solid powder form using freeze dryer at -60 ºC for 72 h. The lyophilized powder was collected and used for further solid-state characterization.

Characterization of nanosuspension

The mean particle size and PDI of freshly prepared nanosuspensions were determined by Dynamic Light Scattering method using the Zetasizer (Nano ZS, Malvern Instruments). The surface charge of nanoparticles was analyzed by measuring the zeta potential in a Zetasizer (Nano ZS, Malvern Instruments, UK). Prior to analysis the samples were diluted with de-ionized water. Three dimensional (3D) images of optimized nanosuspension were obtained by using an Atomic Force Microscope (AFM Shimadzu WET-SPM 9600, Tyoto Japan). Surface morphology and topography of the optimized nanosuspension was evaluated by using scanning electron microscope (JEOL, JSM-6400, Japan) at an accelerating voltage of 10.0 KV under different magnifications. The molecular interactions of optimized nanosuspension with stabilizer were recorded on an FT-IR spectrometer (Perkin Elmer Spectrum Version 10.4.3). For this purpose, coarse plant extract, formulated nanosuspension and SLS (stabilizer) were subjected to FT-IR analysis. The spectra were obtained in KBr disk. A small amount of sample

was placed on the lens and scans were obtained with scanning range between 4000 - 450 cm^{-1}.

Dissolution study

The *in vitro* dissolution profile of coarse suspension and optimized nanosuspension were determined in a phosphate buffer (pH 7.4) using USP Apparatus-2 (paddle method). The lyophilized nanosuspension powder (200mg) was placed in 900 mL dissolution medium at 37 °C with constant stirring at 100 rpm. After specific time intervals (10, 20, 30, 50, 60, 90 and 120 minutes), 5 ml of dissolution medium was collected and replaced with the equal volume of fresh dissolution medium to maintain the constant volume of the dissolution medium. Silybin in *S. marianum* coarse suspension and nanosuspension was analyzed spectrophotometrically at 288 nm as silybin flavonoids give strong absorbance at this wavelength [15]. The dissolution test was conducted in triplicate and results are expressed as mean ± S.D (n = 3).

Statistical analysis

For process optimization of nanosuspensions, CCD was used and data analyzed using Design Expert Software (version 7.1, Stat-Ease, Inc. USA). Results of dissolution studies were expressed as mean ± SD.

RESULTS

Optimized process parameters for *S. marianum* nanosuspensions

CCD was employed to study the impact of selected parameters on mean particle size, PDI and zeta potential values of nanosuspensions. The Design-Expert software was used for predicting the best fitted model, and quadratic polynomial regression equations were constructed by means of regression analysis. Response surface plots were generated to explore the main effects and relationship between independent and dependent variables. Total of 20 formulations were prepared according to experimental design and characterized for particle size, PDI and zeta potential. The optimized nano-formulation was selected on the basis of smallest mean particle size, lower PDI and required zeta potential values. The experimental design used for optimization with observed responses for twenty experiments are presented in Table 1. The second order polynomial regression equation showing the impact of S/PE ratio (A), AS/S ratio (B) and stirring time (C) on mean particle size, PDI and zeta potential are represented as in Eqs 1 - 3.

Mean particle size **(Y_1)** = 197.78 + 20.12A - 38.51B - 16.08C + 6.96AB - 6.84AC - 1.39BC - $0.14A^2 – 3.60B^2 + 21.25C^2$ ……. (1)

PDI **(Y_2)** = 0.37 + 0.020A - 0.044B - 0.025C - 0.013AB + 6.375E- 003ACb - 4.625E-003BC + $0.024A^2 – 5.722E\text{-}004B^2 + 0.017C^2$ …… (2)

Zeta potential **(Y_3)** = 32.86 + 4.24A + 1.45B + 4.57C - 1.61AB + 0.19AC + 1.99BC + $1.90A^2$ + $0.18B^2$ - $0.67C^2$ ……. (3)

The positive sign represent a synergistic effect while the negative sign indicates an antagonistic effect of the variables on response. The analysis of variance (ANOVA) has been employed to determine the significance of selected model. The statistical significance of regression models was determined by F-value which is a measurement of variation of experimental data about the mean. The ANOVA Table of quadratic models for mean particle size, PDI and zeta potential of *S. marianum* nanosuspensions are presented in Table 2, Table 3 and Table 4. The higher model F-values of 35.85 (for mean particle size), 11.90 (for PDI) and 17.41 (for zeta potential) indicated that the proposed quadratic models were good predictors of the experimental data. Values of Prob > F lower than 0.05 (< 0.0001 for Y_1, 0.0003 for Y_2, < 0.0001 for Y_3) revealed that the models were significant.

The Lack of Fit F-value of 0.0783 (for Y_1), 0.5859 (for Y_2) and 0.4830 (for Y_3) implied that lack of fit is insignificant relative to pure error. The insignificant lack of fit confirmed the correctness of selected models. The coeffcient of determination (R^2) of 0.9699, 0.9146 and 0.9400 for particle size, PDI and zeta potential showed a good correlation between experimental and predicted values. The value of R^2_{adj} 0.9363 (Y_1), 0.8566 (Y_2) and 0.8900 (Y_3) were close to R^2 suggesting the high significance of the model. The adequate precision values for three responses obtained were 21.842 (Y_1), 13.043 (Y_2) and 15.038 (Y_3) indicating adequate signal. Furthermore, lower values of CV for all three responses indicated the accuracy and reliability of the experiments.

The effect of input variables on response variables was also explored by generating 3D response surface plots. Figure 1 (a) reveals the combined effect of S/PE ratio and AS/S ratio on particle size with stirring time constant at 4 h. The mean particle size was increased by

increasing S/PE ratio and decreased by increasing AS/S ratio. The minimum particle size of 125 nm was obtained in formulation S1 prepared with low S/PE ratio (1:1) and high AS/S ratio (15:1). The response surface plot in Figure 1 (b) exhibits the interaction effect of S/PE ratio and stirring time on mean particle size at fixed level of AS/S ratio. Figure 1(b) clearly illustrating that mean particle size was decreased by increasing stirring time and increased by increasing S/PE ratio. The plot in Figure 1 (c) reveals the interaction effect of AS/S ratio and stirring time at fixed level of S/PE ratio. Graph indicates significant reduction in mean particle size by increasing AS/S ratio and stirring time up to an optimum value. Further increase in stirring time, however, increased the particle size.

The interaction effect of S/PE ratio and AS/S ratio on PDI values of *S. marianum* nanosuspensions at fixed stirring time is given in Figure 2 (a). The graph clearly demonstrates that PDI first decreased and then increased with increasing S/PE ratio. By increasing the AS/S ratio PDI values of *S. marianum* nanosuspensions were decreased. Figure 2 (b) illustrates the interaction effect of S/PE ratio and stirring time at fixed value of AS/S ratio.

Table 1: Effect of process variables on particle size, PDI and zeta potential of *S. marianum* nanosuspensions

Formulation code	S/PE ratio	AS/S ratio	Time (h)	Particle size (nm)	PDI	Zeta potential (-mV)
S1	1	15	6	125.0	0.325	41.0
S2	2.2	15	6	180.9	0.332	44.2
S3	0.59	10	4	179.7	0.385	29.3
S4	1.6	10	4	195	0.359	36.5
S5	1	5	2	240.3	0.451	24.4
S6	1.6	10	4	190	0.366	32.1
S7	1.6	18.4	4	134.9	0.303	34.6
S8	1.6	10	4	194.0	0.362	33
S9	2.61	10	4	224.8	0.497	47.6
S10	1	15	2	152.0	0.393	27.8
S11	1.6	10	4	198.0	0.352	31.5
S12	2.2	15	2	223.4	0.375	31.7
S13	1.6	10	0.64	290	0.469	23.2
S14	1.6	1.59	4	250	0.438	32.6
S15	1.6	10	7.36	235.5	0.372	39.2
S16	1.6	10	4	210	0.412	30.6
S17	1.6	10	4	198	0.345	33.4
S18	2.2	5	2	295.7	0.486	34.8
S19	1	5	6	230.7	0.401	29.7
S20	2.2	5	6	246.9	0.462	39.3

Table 2: ANOVA statistical data for particle size of *S. marianum* nanosuspensions

Source	Sum of Squares	df	Mean Square	F-value	*P*-value Prob > F	
Model	37112.75	9	4123.64	35.85	< 0.0001	Significant
A-S/PE ratio	5527.40	1	5527.40	48.05	< 0.0001	Significant
B-AS/S ratio	20249.45	1	20249.45	176.03	< 0.0001	Significant
C-Time	3529.77	1	3529.77	30.68	0.0002	Significant
AB	387.81	1	387.81	3.37	0.0962	
AC	374.01	1	374.01	3.25	0.1015	
BC	15.40	1	15.40	0.13	0.7221	
A^2	0.26	1	0.26	2.303E-003	0.9627	
B^2	186.81	1	186.81	1.62	0.2314	
C^2	6510.28	1	6510.28	56.59	< 0.0001	Significant
Residual	1150.33	10	115.03			
Lack of fit	918.83	5	183.77	3.97	0.0783	Not significant
Pure error	231.50	5	46.30			
Cor total	38263.09	19				
R^2		0.9699		Pred R^2		0.8063
Adj R^2		0.9429		C.V. %		5.11
Adeq Precision		21.842				

The sign E in above table stands for exponent

Table 3: ANOVA statistical data for PDI of *S. marianum* nanosuspensions

Source	Sum of Squares	df	Mean Square	F-value	*P*-value Prob > F	
Model	0.055	9	6.086E-003	11.90	0.0003	Sig
A-S/PE ratio	5.472E-003	1	5.472E-003	10.70	0.0084	Sig
B-AS/S ratio	0.027	1	0.027	51.88	<0.0001	Sig
C-Time	8.874E-003	1	8.874E-003	17.35	0.0019	Sig
AB	1.431E-003	1	1.431E-003	2.80	0.1254	
AC	3.251E-004	1	3.251E-004	0.64	0.4439	
BC	1.711E-004	1	1.711E-004	0.33	0.5758	
A^2	8.547E-003	1	8.547E-003	16.71	0.0022	Sig
B^2	4.719E-006	1	4.719E-006	9.225E-003	0.9254	
C^2	4.217E-003	1	4.217E-003	8.24	0.0116	Sig
Residual	5.116E-003	10	5.116E-004			
Lack of fit	2.298E-003	5	4.596E-004	0.82	0.5859	NS
Pure error	2.818E-003	5	5.636E-004			
Cor total	0.060	19				
R^2			0.9146	Adj R^2		0.8377
Pred R^2			0.6411	C.V%		5.74
Adeq Precision			13.043			

Note: Sig = significant, NS = not significant

Table 4: ANOVA statistical data for zeta potential of *S. marianum* nanosuspension

Source	Sum of squares	df	Mean square	F-value	*P*-value Prob > F	
Model	674.57	9	74.95	17.41	<0.0001	Sig
A-S/PE ratio	245.28	1	245.28	56.97	<0.0001	Sig
B-AS/S ratio	28.89	1	28.89	6.71	0.0269	Sig
C-Time	285.19	1	285.19	66.24	<0.0001	Sig
AB	20.80	1	20.80	4.83	0.0526	
AC	0.28	1	0.28	0.065	0.8034	
BC	31.60	1	31.60	7.34	0.0220	Sig
A^2	51.79	1	51.79	12.03	0.0060	Sig
B^2	0.47	1	0.47	0.11	0.7475	
C^2	6.42	1	6.42	1.49	0.2499	
Residual	43.05	10	4.31			
Lack of fit	21.96	5	4.39	1.04	0.4830	NS
Pure error	21.10	5	4.22			
Cor total	717.62	19				
R^2			0.9400	Adj R^2		0.8860
Pred R^2			0.7253	C.V%		6.13
Adeq Precision			15.038			

Note: Sig = significant, NS = not significant

A sharp decreasing trend in PDI values of *S. marianum* nanoformulations was observed by increasing stirring time and S/PE ratio. Moreover, PDI values of *S. marianum* nanosuspensions were decreased by increasing AS/S ratio and stirring time at fixed level of S/PE ratio (Figure 2 c). Figure 3(a) shows the interaction effect of S/PE ratio and AS/S ratio on zeta potential values of nanosuspensions at fixed value of stirring time. Zeta potential of *S. marianum* nanosuspensions were increased by increasing S/PE ratio. However, AS/S ratio has no significant effect on zeta potential values of *S. marianum* nanoformulations.

Validation of model

To optimize all the responses (mean particle size, PDI, zeta potential) numerical optimization using desirability and graphical optimization technique by using overlay plot was used (Figure 4). The optimized nanosuspension of *S. marianum* seeds extract was obtained after setting the constrains on independent and response variables. The levels of input variables which minimize the mean particle size (Y_1), PDI (Y_2) and maximize zeta potential (Y_3) were calculated by Design Expert software for achieving optimized formulation. The optimum values of input variables caluculated from softaware were A (1:1), B (15:1) and C (6 h) to obtain the particle size (139.08 nm), PDI (0.319) and zeta potential (-39 mV). The fresh formulation was prepared and evaluated for particle size, PDI and zeta potential. The optimized formulation with mean particle size of 137 nm, PDI of 0.327 (Figure 5 a) and zeta potential of -37 mV (Figure 5 b) was obtained.

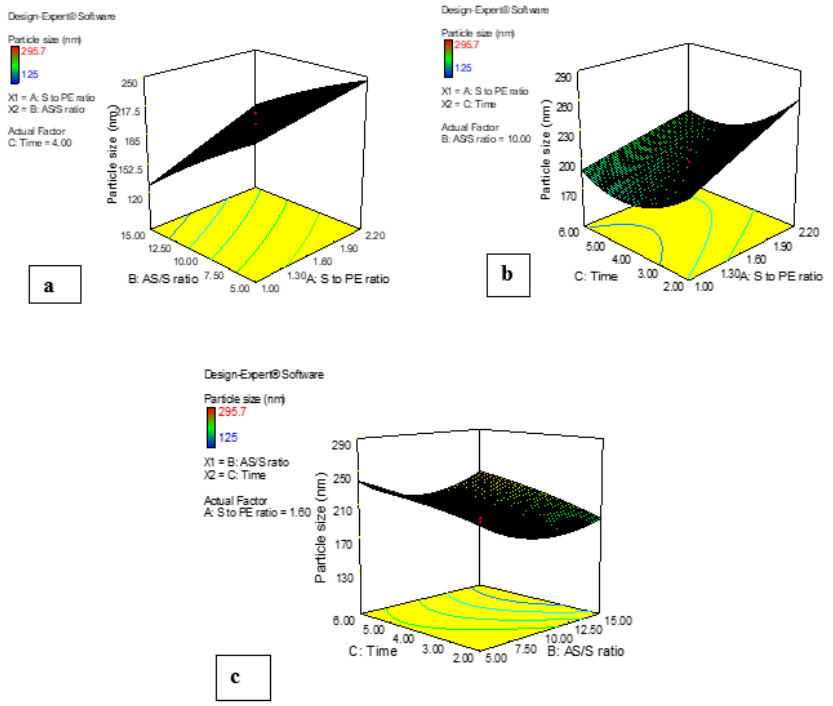

Figure 1: 3D response surface plots showing the effect of (a) S/PE ratio and AS/S ratio (b) S/PE ratio and stirring time (c) AS/S ratio and stirring time on mean particle size of *S. marianum* nanosuspensions

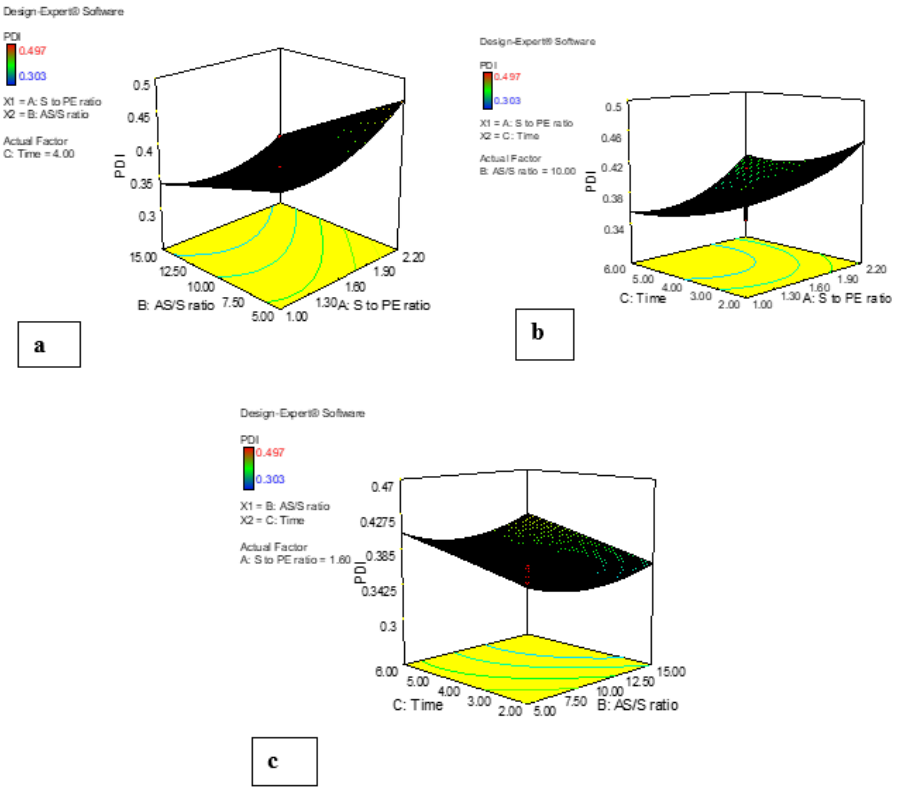

Figure 2: 3D response surface plots showing the effect of (a) S/PE ratio and AS/S ratio (b) S/PE ratio and stirring time (c) AS/S ratio and stirring time on PDI values of *S. marianum* nanosuspensions

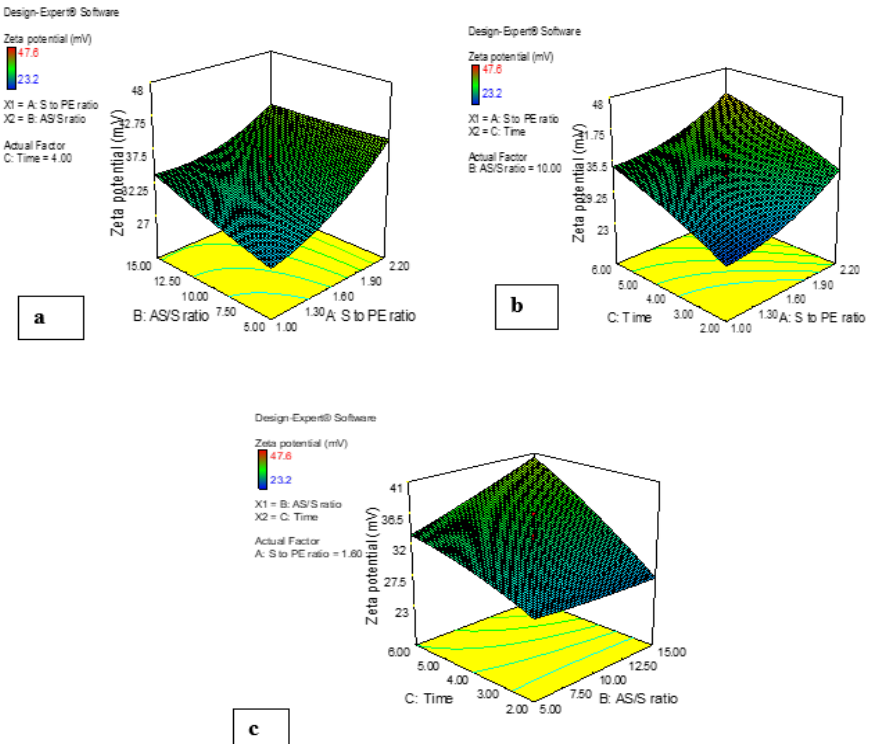

Figure 3: 3D response surface plots showing the effect of (a) S/PE ratio and AS/S ratio (b) S/PE ratio and stirring time (c) AS/S ratio and stirring time on zeta potential of *S. marianum* nanosuspensions

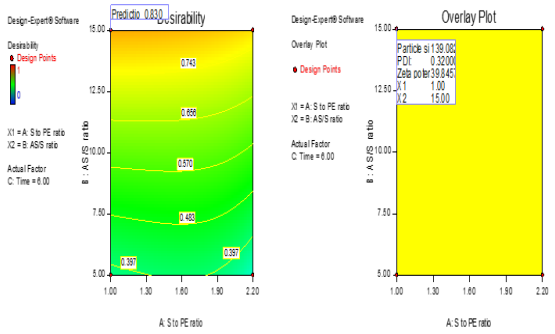

Figure 4: Desirability and overlay plot for optimization of *S. marianum* nanosuspensions

Stability studies

Physical stability of optimized nanosuspension of *S. marianum* extract was determined at room temperature and 4 ºC for the period of three months. The appearance, mean particle size, PDI and zeta potential were recorded after three months. No visual sedimentation of particles was observed at the two different temperatures after subsequent period. It was found that mean particle size, PDI and zeta potential of *S. marianum* optimized nanosuspension was slightly increased after the storage period (Table 5). These results indicated that nanosuspension formulation maintained the particle size during storage conditions.

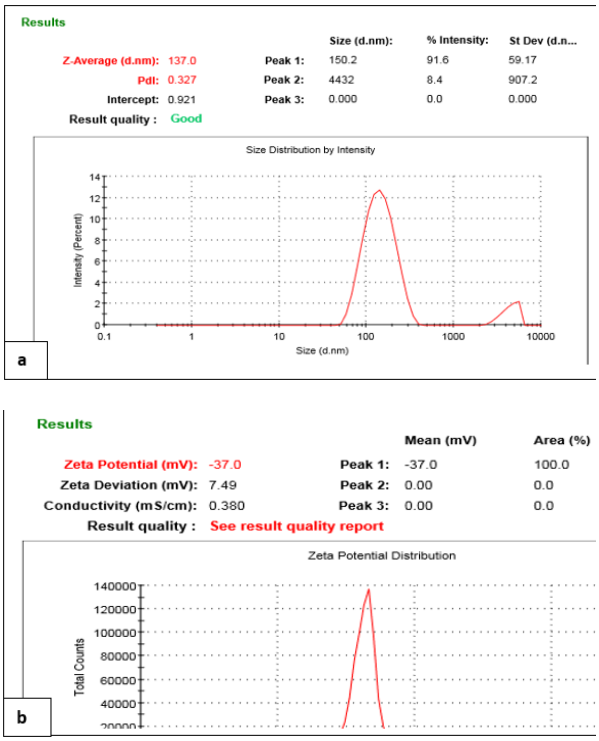

Figure 5: (a) Mean particle size, PDI and (b) zeta potential of optimized nanosuspension of *S. marianum* seeds extract

Table 5: Stability of *S. marianum* optimized nanosuspension

Storage temperature (ºC)	Mean particle size (nm)	PDI	Zeta potential (mV)
25	152.8	0.387	-33.5
4	144.1	0.333	-34.6

Atomic force microscopic (AFM) features

Atomic Force microscopic features confirmed the mean particle size of optimum formulation in nanometer range. In AFM technique the size of particles evaluated as height of the particles. Particles were spherical in shape with average height 298.26 nm. The height of particles measured in scale A-B were 29.9 and 71.98 nm (Figure 6). The great difference in sizes of particles indicated non-uniform particle size distribution. Agglomeration of particles was also observed which might be due to drying step during sample preparation.

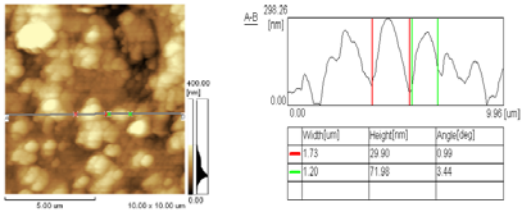

Figure 6: AFM image of *S. marianum* nanosuspension

Scanning electron microscopy

SEM image of nanosuspension of *S. marianum* extract revealed aggregates of irregular shaped particles (Figure 7).

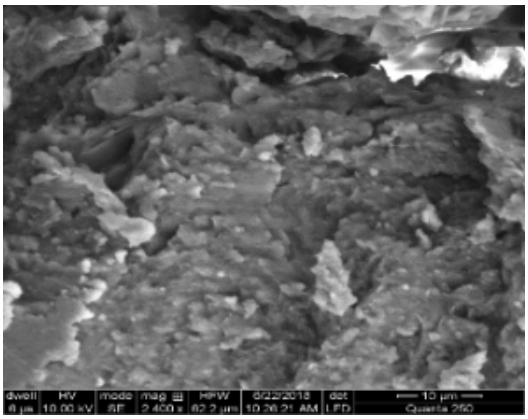

Figure 7: SEM image of *S. marianum* nanosuspension

FT-IR spectra

The FT-IR spectra of *S. marianum* extract, optimized nanosuspension and SLS (stabilizer used for formulation of nanosuspension) are given in Figure 8(a-c) respectively. A broad peak at 3445.26 cm^{-1} in recorded spectrum of *S. marianum* extract was assigned to –OH stretching vibration. A recorded FT-IR spectrum of nanosuspension exhibited the characteristc peak of –OH stretching in this region with slight variation in position and intensity indicating hydrogen bonded interaction between phenolic –OH and stabilizers. Other peaks in spectrum of *S. marianum* extract was observed at 2917.33 (–CH stretching vibration) and 1638.59 cm^{-1} (stretching vibration of –CO group). In spectrum of nanosuspension, these peaks were shifted to higher wavenumber. In addition, the more intensity of these peaks in nanosuspension indicated some minor intermolecular interactions between plant bioactive and stabilizer.

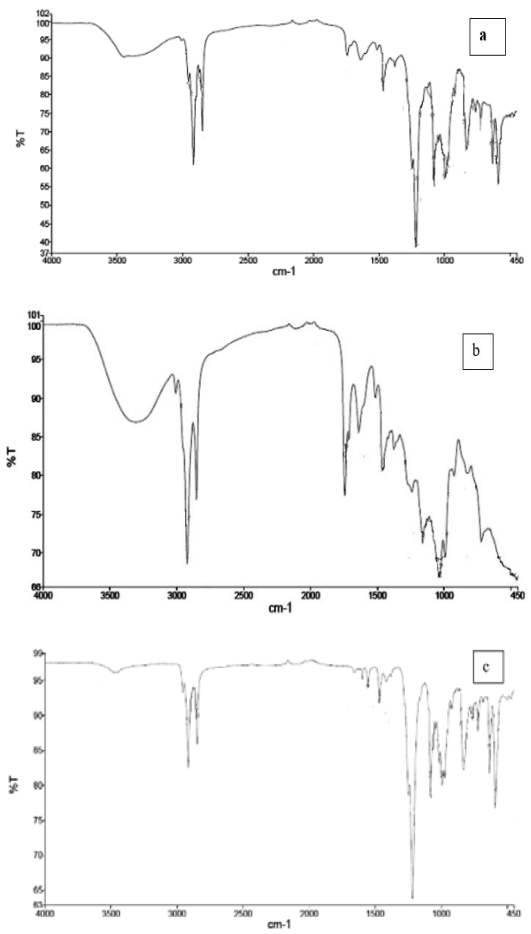

Figure 8: FT-IR spectra of (a) *S. marainum* extract (b) *S. marainum* nanosuspension and (c) SLS

Dissolution

The dissolution profile of optimized *S. marianum* nanosuspension (NS) and coarse suspension (CS) are given in Figure 9. In first ten minutes, approximately 41.41% *S. marianum* nano-suspension and 21.5% coarse suspension (silybin equivalent) were dissolved in dissolution medium. The dissolution velocity of *S. marianum* NS and CS was increased with time. The presented results in graph illustarted that the dissolution of *S. marianum* NS was faster than CS at every time point. After 120 min, 95.78% silybin was released from lyophilized *S. marianum* nanosuspension. In contrast to this only 58.12% of silybin was released from *S. marianum* CS into phosphate buffer.

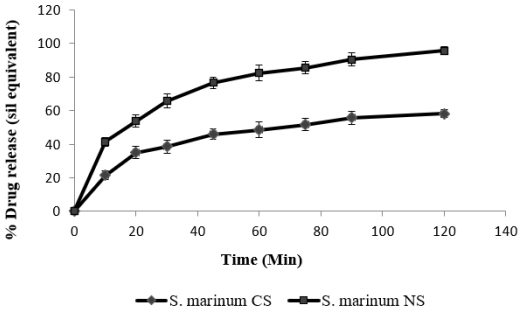

Figure 9: Dissolution profile of *S. marianum* nanosuspension and coarse suspension. Results are expressed as mean ± SD (n = 3), Sil: Silybin NS: Nanosuspension, CS: Coarse suspension

DISCUSSION

In the present study, nanosuspension of *S. marianum* extract was formulated by using antisolvent precipitation method and different parameters were optimized by using response surface methodology. From 3D response surface plots, increase in mean particle size with increasing S/PE ratio indicated that low concentration of stabilizer was sufficient for providing electrostatic repulsion between nanoparticles. Further increasing the amount of SLS increased the free surfactant in solution forming the SLS micelles. The increased solubility of plant phytoconstituents in SLS micelles promotes Ostwald ripening leading to increase in particle size [16].

Moreover, increase in concentration of SLS above the required value increased the osmotic pressure in the solution, which caused the attraction between colloidal particles, leading to the formation of larger particles [17]. By increasing AS/S ratio, the particle size was decreased due to decreased solubility of plant extract in antisolvent and higher supersaturation rate [18]. The reduction in mean particle size by increasing stirring time is attributed to the increased mechanical energy provided for generating smaller particles. But further increase in stirring time above an optimum value resulted in increase in particle size due to enhanced collisions between nanoparticles, leading to aggregation [19].

The reduction in PDI values by increasing S/PE ratio revealed that higher SLS concentration favors the production of more uniform particle size distribution. But further increase in stabilizer concentration results in Ostwald ripening and growth of nanosized particles. Zeta potential is the potential measured at hydrodynamic shear plane and measured by determining the electrophoretic mobility under an electric field. The electrophoretic mobility depends upon surface charge and concentration of electrolyte. The main mechanism of electrostatic stabilization by surfactants is due to ionic interaction on the drug surface. The high surface charge caused electrostatic repulsion; thus, prevent the nanoparticles from agglomeration and aggregation [20]. It was found that the observed values of response variables were in good agreement with the values predicted by the model. These results showed that that model was reliable for predicting the effect of selected variables on response variables.

The results of dissolution study suggested that enhanced dissolution velocity of *S. marianum* nanosuspension is due to reduced particle size. The reduced particle size and high surface area of nanoparticles significantly increased saturation solubility and dissolution velocity of nanosuspensions [21]. The saturation solubility was strikingly enhanced by reducing the particle size according to Ostwald-Freundlich equation [22]. The enhanced dissolution rate of nanosuspensions by decreasing particle size was explained by *Noyes Whitney* equation [23]. The enhanced dissolution rate of nanosuspensions could also be explained due to increased solubility and wettability of poorly soluble flavonoids of plant extract in dissolution medium, due to presence of surface stabilizers [24].

CONCLUSION

Nanosuspension of *S. marianum* seeds extract has been successfully formulated by anti-solvent precipitation method. The optimized formulation has a mean particle size of 137 nm, PDI of 0.327, zeta potential of -37 mV and is stable for three months at room temperature and in refrigerator. The optimized formulation exhibits

remarkable enhancement in dissolution velocity when compared to coarse suspension. Thus, nanosuspensions is potentially a suitable pharmaceutical formulation for poorly soluble herbal extracts.

DECLARATIONS

Acknowledgements

None provided.

Funding

None provided.

Ethical approval

None provided.

Availability of data and materials

The datasets used and/or analyzed during the current study are available from the corresponding author on reasonable request.

Conflict of Interest

No conflict of interest associated with this work.

Contribution of Authors

The authors declare that this work was done by the authors named in this article and all liabilities pertaining to claims relating to the content of this article will be borne by them. Fareeha Kousar conducted the entire research work and wrote the manuscript. Nazish Jahan suggested the plan of the work, supervised the whole project and improved the manuscript. Bushra Sultana and Khalil-Ur-Rahman contributed in manuscript editing and provided research facilities.

REFERENCES

1. *Celik HT, Guru M. Extraction of oil and silybin compounds from milk thistle seeds using supercritical carbon dioxide. J Supercrit Fluids 2015; 100: 105-109.*
2. *Kumar N, Rai A, Reddy ND, Raj PV, Jain P, Deshpande P, Mathew G, Kutty NG, Udupa N, Rao CM. Silymarin liposomes improves oral bioavailability of silybin besides targeting hepatocytes and immune cells. Pharmacol Rep 2014; 66: 788-798.*
3. *Younis N, Shaheen MA, Abdallah MH. Silymarin-loaded Eudragit RS100 nanoparticles improved the ability of silymarin to resolve hepatic fibrosis in bile duct ligated rats. Biomed Pharmacother 2016; 81: 93–103.*
4. *Yin T, Zhang Y, Liu Y, Chen Q, Fu Y, Liang J, Zhou J, Tang X, Liu J, Huo M. The efficiency and mechanism of N-octyl-O, N-carboxymethyl chitosan-based micelles to enhance the oral absorption of silybin. Int J Pharm 2018; 536: 231–240.*
5. *Kocbek P, Baumgartner S, Kristl J. Preparation and evaluation of nanosuspensions for enhancing the dissolution of poorly soluble drugs. Int J Pharm 2006; 312: 179-186.*
6. *Han X, Wang M, Ma Z, Xue P, Wang Y. A new approach to produce drug nanosuspensions CO2-assisted effervescence to produce drug nanosuspensions. Colloids Surf B: Biointerfaces 2016; 143: 107-110.*
7. *Singh MK, Pooja D, Ravuri HG, Gunukula A, Kulhari H, Sistla R. Fabrication of surfactant-stabilized nanosuspension of naringenin to surpass its poor physicochemical properties and low oral bioavailability. Phytomedicine 2018; 40: 48-54.*
8. *Hu L, Yang C, Kong D, Hu Q, Gao N, Zhai F. Development of a long-acting intramuscularly injectable formulation with nanosuspension of andrographolide. J Drug Deliv Sci Technol 2016; 35: 327-332.*
9. *Tang X, Fu Y, Meng Q, Li L, Ying X, Han M, He Q, Yang B, Zeng S, Hu Y, et al. Evaluation of pluronic nanosuspensions loading a novel insoluble anticancer drug both in vitro and in vivo. Int J Pharm 2013; 456: 243-250.*
10. *Wang Y, Zheng Y, Zhang L, Wang Q, Zhang D. Stability of nanosuspensions in drug delivery. J Control Release 2013; 172: 1126-1141.*
11. *Geng T, Banerjee P, Lu Z, Zoghbi A, Li T, Wang B. Comparative study on stabilizing ability of food protein, non-ionic surfactant and anionic surfactant on BCS type II drug carvedilol loaded nanosuspension: Physicochemical and pharmacokinetic investigation. Eur J Pharm Sci 2017; 109: 200-208.*
12. *Wang Y, Liu Z, Zhang D, Gao X, Zhang X, Duan C, Jia L, Feng F, Huang Y, Shen Y, et al. Development and in vitro evaluation of deacety mycoepoxydiene nanosuspension. Colloids Surf B: Biointerfaces 2011; 83: 189-197.*
13. *Gao L, Zhang D, Chen M, Duan C, Dai W, Jia L, Zhao W. Studies on pharmacokinetics and tissue distribution of*

oridonin nanosuspensions. Int J Pharm 2008; 355: 321–327.

14. *Steffi PF, Srinivasan M. Preparation, characterization and stabilization of curcumin nanosuspension. Int J pharmtech res 2014; 6 (2): 842-849.*
15. *Hong C, Dang Y, Lin G, Yao Y, Li G, Ji G, Shen H, Xie Y. Effects of stabilizing agents on the development of myricetin nanosuspension and its characterization: An in vitro and in vivo evaluation. Int J Pharm 2014; 477: 251–260.*
16. *Mishra B, Sahoob J, Dixit PK. Formulation and process optimization of naproxen nanosuspensions stabilized by hydroxy propyl methyl cellulose. Carbohydr Polym 2015; 127: 300-308.*
17. *Yu P, Lu S, Zhang S, Zhang W, Li Y, Liu J. Enhanced oral bioavailability and diminished food effect of lurasidone hydrochloride nanosuspensions prepared by facile nanoprecipitation based on dilution. Powder Technol 2017; 312: 11–20.*
18. *Zu Y, Wu W, Zhao X, Li Y, Wang W, Zhong C, Zhang Y, Zhao X. Enhancement of solubility, antioxidant ability and bioavailability of taxifolin nanoparticles by liquid antisolvent precipitation technique. Int J Pharm 2014; 471: 366–376.*
19. *Ahuja BK, Jena SK, Paidi SK, Bagri S, Suresh S. Formulation, optimization and in vitro–in vivo evaluation of febuxostat nanosuspension. Int J Pharm 2015; 478:540-552.*
20. *George M, Gosh I. Identifying the correlation between drug/stabilizer properties and critical quality attributes (CQAs) of nanosuspension formulation prepared by wet media milling technology. Eur J Pharm Sci 2013; 48: 142-152.*
21. *Li Y, Zhao X, Zu Y, Zhang Y. Preparation and characterization of paclitaxel nanosuspension using novel emulsification method by combining high speed homogenizer and high-pressure homogenization. Int J Pharm 2015; 490: 324–333.*
22. *Santos AMD, Carvalho FC, Teixeira DA, Azevedo DL, Barros WMD, Gremiao MPD. Computational and experimental approaches for development of methotrexate nanosuspensions by bottom-up nanoprecipitation. Int J Pharm 2017; 524: 330-338.*
23. *Al-Kassas R, Bansal M, Shaw J. Nanosizing techniques for improving bioavailability of drugs. J Control Release 2017; 260: 202-212.*
24. *Guo J, Yue P, Lv J, Han J, Fu S, Jin S, Jin S, Yuan H. Development and in vivo/in vitro evaluation of novel herpetrione nanosuspension. Int J Pharm. 2013; 441: 227– 233.*